Causality Mapping Using Resting-State fMRI reveals Suppressed Functional Connectivity in Schizophrenia Patients

Fayyaz Ahmed[1], Zunira Saghir[1], Namra Aamir[2], Turki Abualait[3], Safee Ullah Chaudhary[2*], Shahid Bashir[4*]

[1] Department of Statistics, University of Gujrat, Gujrat, Pakistan,

[2] Biomedical Informatics Research Laboratory, Department of Biology, Syed Babar Ali School of Science and Engineering, Lahore University of Management Sciences, Lahore, Pakistan,

[3] College of Applied Medical Sciences, Imam Abdulrahman Bin Faisal University, Dammam, Saudi Arabia,

[4] Neuroscience Center, King Fahad Specialist Hospital Dammam, Dammam, Saudi Arabia.

Short running title: Causality Mapping and Schizophrenia

***Correspondence**:

Safee Ullah Chaudhary
Biomedical Informatics Research Laboratory, Department of Biology, Syed Babar Ali School of Science and Engineering, Lahore University of Management Sciences, Lahore, Pakistan
ORCID No: https://orcid.org/0000-0002-3758-6581
Email: safee.ullah.chaudhary@gmail.com

Shahid Bashir *
Neuroscience Center, King Fahad Specialist Hospital Dammam, Dammam, Saudi Arabia.
P.O. Box 15215, Dammam 31444, Saudi Arabia
ORCID No: https://orcid.org/0000-0001-6286-6895
E-mail: sbashir10@gmail.com

Tel.: +966 13 8442222 (Ext. 2423)

Keywords: Granger causality analysis, migraine, pain-related networks, resting-state functional magnetic resonance imaging

ABSTRACT

Schizophrenia is a psychotic brain disorder in which patients exhibit aberrant connectivity between different regions of the brain. Neuroimaging is a state-of-the-art technique that is now increasingly been employed in clinical investigation of Schizophrenia. In the present study, we have used resting-state functional magnetic resonance neuroimaging (rsfMRI) to elucidate the cause-and-effect relationships among four regions of the brain including occipital, temporal, and frontal lobes and hippocampus in Schizophrenia. For that, we have employed independent component analysis, a seed-based temporal correlation analysis, and Granger causality analysis for measuring causal relationships amongst four regions of the brain in schizophrenia patients. Eighteen subjects with nine patients and nine controls were evaluated in the study. Our results show that Schizophrenia patients exhibit significantly different activation patterns across the selected regions of the brain in comparison with the control. In addition to that, we also observed an aberrant causal relationship between these four regions of the brain. In particular, the temporal and frontal lobes of patients with schizophrenia had a significantly lowered causal relationship with the other areas of the brain. Taken together, the study elucidates the dysregulated brain activity in Schizophrenia patients, decodes its causal mapping and provides novel insights towards employment in clinical evaluation of Schizophrenia.

INTRODUCTION

Schizophrenia (SZ) is a chronic mental disorder affecting approximately 1% of the global population (1). The condition is characterized by cognitive and behavioral alterations, accompanied by hallucinations, delusions, and disorganized thinking (2,3). SZ typically develops in young adults between the age of 18 and 35 (4) and has a lifetime prevalence of 1% (4). Recent research on SZ has uncovered several genetic and environmental factors that correlates with the development of the disease (4). An increasing amount of experimental evidence is now suggesting that SZ induces extensive alterations in the connectivity between various regions of the brain that results in its functional dysregulation (5,6). Moreover, research studies have also reported significant reductions in functional connectivity amongst various regions of the brain in SZ patients (7–9). However, the type and scale of these disconnections, suppressed functional connectivity and the underlying pathophysiological mechanisms in SZ remain unclear (11).

Advancements in brain imaging techniques and protocols have now enabled scientists to carry out in-depth investigations of the neuropathological mechanisms of SZ (10–14). Several groundbreaking studies leveraging these technologies have helped reveal a wide variety of abnormal structural and functional connections among anatomically distant regions of the brain in SZ patients (15–18). Investigations using functional brain imaging have helped elucidate reduced activation in the frontal, striatal, and parietal regions during the performance of cognitive tasks in patients with SZ (19,20). Furthermore, altered patterns of neural activation have been reported in the prefrontal cortices, including the anterior cingulate cortex (ACC), the supplementary motor area (SMA), the pre-SMA, the parietal cortex, and the subcortical basal ganglia nuclei (20–23). Data from diffusion tensor imaging have highlighted reduced fractional anisotropy (FA) in the internal capsule, thalamus, corpus callosum (CC), white matter microstructures (24), and throughout the entire brain in patients with SZ (25). Reduced FA in the CC has been associated with higher lateral ventricle (LV) volume, while higher radial diffusivity (RD) values are associated with larger LV volume in patients with SZ (26). This suggests that SZ may involve abnormalities in structural white matter, which connects and activates different regions of the brain.

These findings have been supported and expanded upon by several neuroimaging studies on functional connectivity (FC), which have elucidated temporal associations

between various regions of the brain (27). Specifically, this approach has been utilized to investigate disruptions in functional connectivity in brain of SZ patients (28). Previous studies have examined specific regions of the brain at resting state (29–31), and during sensory (32), and cognitive tasks (33) in patients with SZ. Reduced FC has been extensively reported in the neural pathways of patients with SZ, including the amygdala subregional-sensorimotor pathway (34), frontotemporal (35), thalamocortical (36), and cortico-cerebellar pathways (37). Differential FC in brain of patients with SZ and healthy controls, therefore, could have significant clinical implications, as psychopharmacological treatments could target aberrant FC in patients with SZ (39, 40). In addition, these differences could also be used as a neuroimaging biomarker to guide diagnoses of SZ (41, 42).

Towards this goal, in this work, we investigate the resting-state functional connectivity in brain of patients with SZ and examine the cause-and-effect relationships among these regions of the brain (38). For that, we have combined three different methods for analyzing FC, including (i) spatial independent component analysis (ICA) to identify the characteristics or features of fMRI data that are maximally independent, (ii) a seed-based temporal correlation analysis (SCA) to assess time-series associations and connections among regions, and (iii) Granger causality analysis (GCA) to analyze effective connectivity in the brain. In specific, spatial ICA is employed to extract the overall connectivity patterns at the whole-brain level and is used to elucidate the spatial structure of the blood-oxygen-level-dependent (BOLD) signal (47, 50, 51). The seed-based SCA was used to identify regions, or "seeds," that correlate with FC and activity in other seeds or regions using time series of BOLD signals from seed-voxels and other regions (41–44). Lastly, the GCA was used to study the bidirectional effects between two variables in a time series (45) to examine time-lagged causal effects on specific regions of the brain by using time predictions between an fMRI time series (46,47). The approach helped identify the dynamic causal interactions between the four selected regions of the brain. Our results show that the brains of patients with SZ exhibit aberrant activation patterns in the HC, OL, TL, and FL. Moreover, the functional and structural connectivity among these four regions differs significantly in patients with SZ, which has been validated by the VAR models using Granger causality. Last, our causal analysis through mediation revealed significant differences in decision making in patients with SZ.

Taken together, this study expands our understanding of the resting-state FC (rsFC) in patients with SZ at the whole-brain level and reports the aberrations in FC among multiple regions of the brain using a combination of statistical approaches. The study also helps characterize the direction of FC among different regions of the brain and how it differs in patients with SZ from healthy controls (39) thereby providing valuable insights into the neural basis of SZ (39).

METHODOLOGY

2.1 Granger causality

We used a Granger causality (G-causal) test and VAR modeling to analyze the fMRI data. This method determines the causal relationships between two variables. If a variable x has a G-causal relationship with another variable y, then the lag values of x can be used to forecast the future values of y and vice versa. This study examined the causal relationships among four regions of the brain: the frontal, occipital, and temporal lobes and the hippocampus.

Mathematical Formulation of Granger Causality

Consider two random variables Xt, Y_t. Assume a lag length of p. For example, y is occipital lobe and X is temporal lobe. For occipital and temporal lobes, the model could be written as:

$$T_t = c_1 + a_1 T_{t-1} + a_2 T_{t-2} + \ldots a_p T_{t-p} + bO_{t-1} + bO_{t-2} + \ldots bO_{t-p} + e_t$$

Estimate by OLS and test for the following hypothesis:

$$H_0 : \beta_1 = \beta_2 = \ldots\ldots = \beta_p = 0$$
$$H_1 : any \beta \neq 0$$

To check if occipital lobe does granger-cause to temporal lobe or not, here we will take y as a occipital lobe ‘o’ and x as a temporal lobe ‘t’.

Unrestricted sum of squared residual:

$$RSS_1 = \sum_t \hat{a}_t^{\,2}$$

Restricted sum of square residual:

$$RSS_2 = \sum_t \hat{\hat{a}}_t^{\,2}$$

$$F = \frac{(RSS_2 - RSS_1)}{RSS_1 / (T - 2p - 1)}$$

Under general condition, the OLS estimate is given by, $b=\left[\sum_{t=1}^{T}\left(o_t o_t'\right)\right]^{-1}\left[\sum_{t=1}^{T}\left(o_t t_t\right)\right]$ assuming that the (kxk) matrix $\sum_{t=1}^{T}\left(o_t o_t'\right)$ is nonsingular the OLS sample residual for observation t is $u_t = t_t - o_t' b$ .Often the model $t_t - o_t'\beta + \mu_t$ is written in matrix notation as

$T - O\beta + \mu$ Where

$$T_{(T\times 1)}=\begin{bmatrix} t_1 \\ t_2 \\ \vdots \\ t_T \end{bmatrix} \quad O_{(T\times k)}=\begin{bmatrix} o_1' \\ o_2' \\ \vdots \\ o_T' \end{bmatrix} \quad u_{(T\times 1)}=\begin{bmatrix} u_1' \\ u_2' \\ \vdots \\ u_T' \end{bmatrix}$$

Then the OLS estimate in $b=\left[\sum_{t=1}^{T}\left(o_t o_t'\right)\right]^{-1}\left[\sum_{t=1}^{T}\left(o_t t_t\right)\right]$ can be written as

$$b=\left\{\left[o_1, o_2 \ldots o_T\right]\begin{bmatrix} o_1' \\ o_2' \\ \vdots \\ o_T' \end{bmatrix}\right\}^{-1}\left\{\left[o_1, o_2 \ldots o_T\right]\begin{bmatrix} t_1 \\ t_2 \\ \vdots \\ t_T \end{bmatrix}\right\}$$

$$=(O'O)^{-1}(O'T)$$

Similarly, residual can be written as:

$$\hat{u}=t-Ob=t-O(O'O)^{-1}O't=\left[I_T-O(O'O)^{-1}O'\right]t=M_{xy}$$

Where M_x is defined as the following (T x T) matrix $M_x = I_T - O(O'O)^{-1}O'$ .One can readily verify that $M_x = M_x'$ where idempotent $M_x M_x = M_x$ and the orthogonal to the columns of O. M_x X=0 .OLS sample residuals are orthogonal to the explanatory variables in O and population residual can be found by substituting $\hat{u}=M_x(O\beta+u)=M_x u$ .The

difference between the OLS estimate b and the true population parameter β is found by substituting $T = O\beta + \mu$ into $b = \left\{ [o_1, o_2 \ldots o_T] \begin{bmatrix} o_1' \\ o_2' \\ \vdots \\ o_T' \end{bmatrix} \right\}^{-1} \left\{ [o_1, o_2 \ldots o_T] \begin{bmatrix} t_1 \\ t_2 \\ \vdots \\ t_T \end{bmatrix} \right\}$

$$b = (O'O)^{-1} O' \left[O\beta + u \right] = \beta + (O'O)^{-1} Xu$$

Now estimate the F test (Wald test) about beta under assumption. A Wald test of Ho is based on the following results. Consider an (nx1) vector z ~ $N(0, \Omega)$ with non-singular then $Z'\Omega^{-1}Z \sim \chi^2_{(n)}$

$$\begin{aligned} Z'\Omega^{-1}Z &= Z'(p \wedge p')^{-1} z \\ &= z' \left[p' \right]^{-1} \wedge^{-1} p^{-1} z \\ &= [p^{-1} z]' \wedge^{-1} p^{-1} z \\ &= w' \wedge^{-1} w \\ &= \sum_{i=1}^{n} w_i^2 / \lambda_i \end{aligned}$$

Where $w = p^{-1} z$ and w is Gaussian with mean zero and variance $E(ww') = E(p^{-1} zz' [p']^{-1}) = p^{-1} \Omega [p']^{-1} = p^{-1} p \wedge p' [p']^{-1} = \wedge$ .Thus $w' \wedge^{-1} w$ is the sum of squares of n independent normal variables each divided by its variance λ .It accordingly has a χ^2_n distribution as claimed. Applying proposition directly to $Rb \sim N(r, \delta^2 R(O'O)^{-1} R')$ under Ho $(Rb - r)' [\delta^2 R(O'O)^{-1} R']^{-1} (Rb - r) \sim \chi^2_m$

Replacing σ with the estimate s and dividing by the number of restriction gives the Wald form of the OLS F test of a linear hypothesis. $F = (Rb - r)' [s^2 R(O'O)^{-1} R']^{-1} (Rb - r) / m$

$$F = \frac{(Rb - r)' [\delta^2 R(O'O)^{-1} R']^{-1} (Rb - r) / m}{[RSS / (T - K)] \delta^2}$$

The numerator is a χ^2_m variable divided by its degree of freedom while the denominator is χ^2 (T-k) variable divided by its degree of freedom again since b and μ are independent, the numerator and denominator are independent of each other hence

$F - (Rb-r)'[s^2R(O'O)^{-1}R']^{-1}(Rb-r)/m$ has an exact F(m ,T-K) distribution under Ho. Let b denote the unconstrained OLS estimate and let RSS_1 be the residual sum of square resulting from using this estimate. $RSS_1 = \sum_{t=1}^{T}(t_t - o_t'b)^2$ Let b* denote the constrained OLS estimate and RSS_o the residual sum squares from the constrained OLS estimation. $RSS_0 = \sum_{t=1}^{T}(t_t - o_t'b^*)^2$. Then the Wald form of the F test of a linear hypothesis $F = (Rb-r)'[s^2R(O'O)^{-1}R']^{-1}(Rb-r)/m$ can equivalently be calculated as $F = \frac{(RSS_o - RSS_1)/m}{RSS_1/(T-K)}$.

Vector auto regression (VAR) model

VAR models are used for estimating and forecasting in time series data. In multivariate time series analysis, it is one of most easy to use technique. It is known as extension of AR model. One of crucial step in VAR is selection of lags for lag selection we have three criteria's AIC BIC HQIC.

$$t_t = b_{10} - b_{12}o_t + v_{11}t_{t-1} + v_{12}o_{t-1} + \varepsilon_t$$
$$o_t = b_{20} - b_{21}t_t + v_{21}t_{t-1} + v_{22}o_{t-1} + \varepsilon_t$$

In above model 'o' represent the occipital lobe and 't' represent the temporal lobe. VAR models are used for forecasting in time series but we can employ them to check the Granger causality of the variables. One of the important steps in VAR model is the selection of lag length which is based on specific criteria.

Data

The study was approved by the Institutional Review Board of King Khalid University Hospital. The participants included a selection of 15 healthy controls and 15 patients with SZ. From these, we selected 18 subjects (9 controls and 9 patients with SZ). All participants underwent the same number of scans according to our study requirements. The participants were aged 33.14 ± 9.96 (mean ± SD) years. The SZ participants were recruited through local psychiatric clinics, and the controls were recruited from hospital volunteers. All participants provided informed written consent before

participating. All SZ and control subjects were outpatients and had been clinically stable for at least two weeks prior to the study. The SZ participants were diagnosed by a research psychiatrist based on the DSM.IV criteria; the diagnoses were confirmed by a trained research assistant.

Written informed consent was obtained from subjects which was approved by the Institutional Review Board (IRB) at King Khalid University Hospital (KKUH). All procedures were conducted according to the Declaration of Helsinki.

3. RESULTS

3.1. The brains of patients with SZ exhibit aberrant activation patterns in the hippocampus (HC), occipital lobe (OL), temporal lobe (TL), and frontal lobe (FL)

To evaluate differences in brain activation patterns in patients with SZ, we obtained fMRI scans of nine subjects with SZ (**Supplementary Data 1**). Nine clinically healthy individuals were also scanned and used as controls (**Supplementary Data 2**). The resulting fMRI scan data were pre-processed for realignment, spatial normalization, smoothing, and co-registration using statistical parametric mapping (SPM12) (48) (**Figures 1A, B**). We then compared activation levels in four regions of interest (ROIs): the hippocampus (HC), the occipital lobe (OL), the temporal lobe (TL) and the frontal lobe (FL). Brain activation in patients with SZ was compared to that of the controls using two independent sample *t*-tests (49). We found that average brain activity in the two groups differed significantly in the HC ($t(798) = 125.254$, $p < 0.05$), the OL ($t(798) = 43.573$, $p < 0.05$), the TL ($t(798) = 130.784$, $p < 0.05$), and the FL ($t(798) = -9.774$, $p < 0.05$) (**Figure 1C**). We conclude that patients with SZ have significantly less activation in the HC, the OL, and the TL than healthy controls (59). However, we also observed significantly higher activation in the FL of patients with SZ.

3.2. Functional connectivity among the HC, OL, TL, and FL differs significantly in patients with SZ

The human brain is a complex neuronal network with variable levels of FC among different regions. FC gives rise to the physiological functions of different regions of the brain. Having observed significant variation in the activation of the four ROIs, we then evaluated the effect of this activation on the FC among these ROIs (28). To do this, we quantified the FC among the four ROIs by computing the Pearson correlations for the SZ and control groups (Figures 2A, B). For the controls, the highest positive correlation was observed between the FL and the TL ($r = 0.85$, $p < 0.05$) while the lowest positive correlation was between the FL and the OL ($r = 0.63$, $p < 0.05$) (Figure 2A). The smallest negative correlation in the controls was observed between the HC and the TL ($r = -0.06$), while the largest negative correlation was between the HC and the OL ($r = -0.01$). For the SZ groups, the highest positive correlation was

observed between the FL and the TL (r = 0.79, $p < 0.05$), while the lowest positive correlation was between the FL and the OL (r = -0.26) (Figure 2B). The smallest negative correlation was between the HC and the TL (r = 0.17, $p < 0.05$), while the largest negative correlation was between the HC and the OL (r = 0.42, $p < 0.05$). These results indicate that the functional connectivity network is significantly altered in patients with SZ (Figures 2C, D).

3.3 Patients with SZ exhibit aberrant structural connectivity in the ROIs

Next, to investigate the temporal variations in FC patterns (or *effective structural connectivity*) among the four ROIs, we employed the vector auto regression (VAR) model (51) at times t-2, t-1, and t. Between t-1 and t, the HC exhibited strong causal connectivity with the OL ($\hat{\beta}^c$ = 0.15, $p < 0.05$) and with the TL ($\hat{\beta}^c$ = -0.2, $p < 0.05$) in healthy individuals. In patients with SZ, these connections of the HC with the OL and the TL were completely inhibited (Figure 3; Tables 1, 2). The TL also had strong causal connectivity with the HC ($\hat{\beta}^c$ = -0.05, $p < 0.05$) and the OL ($\hat{\beta}^c$ = 0.12, $p < 0.05$) in the controls; these connections were also deregulated in the SZ group. The OL had causal connectivity with the FL ($\hat{\beta}^c$ = 0.78, $p < 0.05$) and vice versa ($\hat{\beta}^c$ = -0.07, $p < 0.05$), and the OL had causal connectivity with the TL ($\hat{\beta}^c$ = 0.09, $p < 0.05$) in the controls; these connections did not appear in patients with SZ. Furthermore, at lag times t-1 and t-2, the HC exhibited significantly diminished FC in patients with SZ. This differed from the controls most remarkably at lag t-2. Interestingly, at t-1 and t-2, the FL and OL showed enhanced anomalous connectivity in patients with SZ. The TL maintained its effective structural connectivity in both the controls and the patients with SZ at lag t-2.

3.4 Validation of VAR models using Granger causality

To validate the structural model of the brain connectivity network obtained through VAR, we further employed a G-causal test (44) to examine the bidirectional causal effects of the ROIs on each other in patients with SZ and in the controls. In the controls (Table 3) the OL and TL regions had significant G-causality with the HC (Figure 4A). Moreover, the HC and the FL were G-causal for OL activation (Figure 4B), while the OL and the FL had G-causality with the TL (Figure 4C). In the controls, the TL also had G-causality with the FL (Figure 4D). However, we observed weaker causal relations among the four ROIs in patients with SZ (Table 4) than in the

controls. Specifically, the HC was not G-causal for the other ROIs in patients with SZ (Figure 4A). However, the TL and the HC continued to have a significant G-causal relationship with the OL (Figure 4B). Moreover, the OL was G-causal for the TL (Figure 4C), while the OL and the TL were G-causal for the FL (Figure 4D). Taken together, these findings confirm our earlier hypotheses on aberrant patterns and reduced activation in the four ROIs in patients with SZ.

3.5 Causal analysis through mediation reveals differences in decision making in patients with SZ

To investigate differences in the decision-making processes of patients with SZ, we performed a causal analysis of HC mediation. To do this, we analyzed the role of the HC as a mediator between the FL and OL in the controls and in patients with SZ (Figure 5). Our results show that the HC played a significant role in the patients with SZ (Figure 5B) but was non-significant in the control group (Figure 5A). We further observed that the FL disturbed the activity of the OL and the HC in patients with SZ, while in the controls this effect was non-significant (Table 5).

4. DISCUSSION

This study examined rsFC in patients with SZ on a whole-brain scale. The results show that the parietal region has less connectivity to bilateral DLPFC, while the parietal and frontal regions have strong connectivity in patients with SZ. Our results also showed that patients with SZ exhibited significantly less activation in the HC, the OL, and the TL than healthy controls (61), while the FL showed significantly more activation in patients with SZ. Abnormal functional connectivity in the prefrontal cortex may reflect psychopathologies such as an inability to allocate internal or external attentional resources, a crucial skill for goal-oriented behaviors (61, 62). Working memory and decision-making deficits have also been repeatedly reported in patients with SZ; these symptoms are often linked to abnormal functioning of the prefrontal cortex (63, 64). Temporal hallucinations and delusions are the main characteristics of SZ; these are mainly attributed to aberrant FC in the temporal cortex (65, 66). There is also a well-established link between SZ and the hippocampus, a complex region of the brain that plays a critical role in multiple cognitive domains, including memory, imagination, and emotions (67, 68), that are known to be impaired in patients with SZ (69).

Approaches such as spatial independent component analysis (ICA), seed-based temporal correlation analysis (SCA) and Granger causality analysis (GCA) can be used to explore the activity and functions of the intrinsic neuronal network using rsfMRI data (70–73). Our findings are consistent with those of other studies. For example, one study by (74) observed reduced degree centrality (DC) of the bilateral putamen nuclei in patients with SZ compared to controls. DC is an index used to identify the regions of the brain (at the whole-brain level) that display functional deficits in patients with SZ. That study also observed a lack of causal connectivity between the putamen and multiple regions of the default mode network (DMN), the orbital area of the inferior frontal cortex, and the right fusiform in patients with SZ. In addition, a previous study found abnormal rsFC in the amygdala subregional-sensorimotor regions of the brain in patients with SZ; this abnormality was also associated with positive symptoms in patients with SZ (75). A similar pattern of altered rsFC has been observed throughout the entire brain in patients with SZ. Disrupted pathways from the limbic areas to the thalamus have also been demonstrated using resting-state effective connectivity (rsEC) analysis (76).

Furthermore, a wide range of alterations to thalamic nuclei functional connectivity have been observed in the cortico-cerebellar-thalamo-cortical circuit pathways of patients with SZ (77). A systematic review of task and rsfMRI studies demonstrated the convergence of brain neural dysfunction between tasks and rsfMRI abnormalities in the prefrontal regions, including the dorsal lateral prefrontal cortex, the orbital frontal cortex, and the TL, particularly the superior temporal gyrus (78). Together, these previous findings demonstrate that patients with SZ exhibit altered FC and effective connectivity (EC) among large regions of the brain. Moreover, brain rsFC and rsEC can be used as diagnostic markers for SZ and might be implicated in therapeutic interventions as well.

A major strength of this study is its use of a combination of three different FC analysis methods to investigate functional disconnections between various regions of the brain. However, the study does have some limitations, which should be considered when interpreting the results. Most significantly, the sample size in the present study is small. Additional longitudinal follow-up studies with larger samples are needed to elucidate the alterations in FC between regions of the brain in patients with SZ.

Conclusion: GCA is a useful tool for characterizing the functional direction of time-series data. GCA has broad implications in the neurosciences and neuroimaging because of the importance of the FC of different regions of the brain during tasks. GCA can be used to characterize the significant functional directions of different regions of the brain. In the above diagram, the functional direction of different regions of the brain are indicated by arrows. These arrows illustrate the significant Granger causes in the patients with SZ (red) and the control subjects (black) in our study. We can conclude that, in patients with SZ, some regions of the brain are less active than those of healthy subjects during task performance.

Ethical publication statement: We confirm that we have read the Journal's position on issues involved in ethical publication and affirm that this report is consistent with those guidelines.

Disclosure

Neither of the authors has any conflict of interest to disclose

Acknowledgements:

The authors would like to thank participants and their family members.

5. REFERENCES

1. Insel TR. Rethinking Schizophrenia Article in Nature. nature.com. 2010 Nov;468(7321):187–93.
2. Author AD-D, 2013 undefined. statistical manual of mental disorders,(DSM-5) Washington.
3. Buckley P, Clinics BM-P, 2015 undefined. Schizophrenia research: a progress report. psych.theclinics.com.
4. Owen MJ, Sawa A, Mortensen PB. Schizophrenia. Lancet. 2016 Jul;388(10039):86–97.
5. Friston K, Brown H, Siemerkus J, research KS-S, 2016 undefined. The dysconnection hypothesis (2016). Elsevier.
6. Stephan K, Baldeweg T, psychiatry KF-B, 2006 undefined. Synaptic plasticity and dysconnection in schizophrenia. Elsevier.
7. Falakshahi H, Vergara V, … JL-IT, 2020 undefined. Meta-modal Information Flow: A Method for Capturing Multimodal Modular Disconnectivity in Schizophrenia. ieeexplore.ieee.org.
8. Han S, Cui Q, Guo X, Fan Y, Guo J, Zong X, et al. Disconnectivity between the raphe nucleus and subcortical dopamine-related regions contributes altered salience network in schizophrenia. Elsevier.
9. Huang C, Luo Q, Palaniyappan L, … AY-BP, 2020 undefined. Transdiagnostic and Illness-specific Functional Dysconnectivity Across Schizophrenia, Bipolar Disorder and Major Depression. Elsevier.
10. Repovs G, Csernansky J, psychiatry DB-B, 2011 undefined. Brain network connectivity in individuals with schizophrenia and their siblings. Elsevier.
11. Fornito A, Zalesky A, Pantelis C, Neuroimage EB-, 2012 undefined. Schizophrenia, neuroimaging and connectomics. Elsevier.
12. Pettersson-Yeo W, Allen P, Benetti S, … PM-N&, 2011 undefined. Dysconnectivity in schizophrenia: where are we now? Elsevier.
13. Abid H, Ahmad F, Lee SY, Park HW, Im D, Ahmad I, et al. A functional

magnetic resonance imaging investigation of visual hallucinations in the human striate cortex. Behav Brain Funct [Internet]. 2016 Nov 29 [cited 2020 Sep 8];12(1). Available from: https://pubmed.ncbi.nlm.nih.gov/27899123/

14. Ahmad F, Hussain A, Chaudhary SU, Ahmad I, Ramay SM. A novel method for detection of voxels for decision making: An fMRI study. Int J Imaging Syst Technol [Internet]. 2016 Jun 1 [cited 2020 Sep 8];26(2):163–7. Available from: http://doi.wiley.com/10.1002/ima.22172

15. Shafiei G, Markello R, Makowski C, … AT-B, 2020 undefined. Spatial patterning of tissue volume loss in schizophrenia reflects brain network architecture. Elsevier.

16. Dong D, Wang Y, Chang X, … CL-S, 2018 undefined. Dysfunction of large-scale brain networks in schizophrenia: a meta-analysis of resting-state functional connectivity. academic.oup.com.

17. Lynall M-E, Bassett DS, Kerwin R, Peter †, Mckenna J, Kitzbichler M, et al. Behavioral/Systems/Cognitive Functional Connectivity and Brain Networks in Schizophrenia. Soc Neurosci. 2010;

18. neuroscience MR-D in clinical, 2013 undefined. Schizophrenia and abnormal brain network hubs. ncbi.nlm.nih.gov.

19. Yoon JH, Minzenberg MJ, Ursu S, Walters R, Wendelken C, Ragland JD, et al. Association of dorsolateral prefrontal cortex dysfunction with disrupted coordinated brain activity in schizophrenia: Relationship with impaired cognition, behavioral disorganization, and global function. Am J Psychiatry. 2008 Aug;165(8):1006–14.

20. Minzenberg MJ, Laird AR, Thelen S, Carter CS, Glahn DC. Meta-analysis of 41 Functional Neuroimaging Studies of Executive Function in Schizophrenia. jamanetwork.com.

21. Snitz BE, MacDonald A, Cohen JD, Cho RY, Becker T, Carter CS. Lateral and medial hypofrontality in first-episode schizophrenia: Functional activity in a medication-naive state and effects of short-term atypical antipsychotic treatment. Am J Psychiatry. 2005 Dec;162(12):2322–9.

22. Sutcliffe G, Harneit A, … HT-BP, 2016 undefined. Neuroimaging intermediate phenotypes of executive control dysfunction in schizophrenia. Elsevier.

23. Vanes L, Mouchlianitis E, Patel K, Barry E, reports KW-S, 2019 undefined. Neural correlates of positive and negative symptoms through the illness course: an fMRI study in early psychosis and chronic schizophrenia. nature.com.

24. Wagner G, Cruz FD la, Schachtzabel C, Cortex DG-, 2015 undefined. Structural and functional dysconnectivity of the fronto-thalamic system in schizophrenia: a DCM-DTI study. Elsevier.

25. White T, Magnotta V, … HB-S, 2011 undefined. Global white matter abnormalities in schizophrenia: a multisite diffusion tensor imaging study. academic.oup.com.

26. Re E Del, Bouix S, Fitzsimmons J, … GB-P, 2019 undefined. Diffusion abnormalities in the corpus callosum in first episode schizophrenia: associated with enlarged lateral ventricles and symptomatology. Elsevier.

27. Friston K, Neurosci CF-C, 1995 undefined. Schizophrenia: a disconnection syndrome. fil.ion.ucl.ac.uk.

28. Bharat Biswal, Zerrin Yetkin Victor M, Haughton James H. Functional connectivity in the motor cortex of resting human brain using echo□planar mri. NCBI. 1995;

29. Liang M, Zhou Y, Jiang T, Liu Z, Tian L, Liu H, et al. Widespread functional disconnectivity in schizophrenia with resting-state functional magnetic resonance imaging. journals.lww.com.

30. Liang S, Li Y, Zhang Z, Kong X, Wang Q, Deng W, et al. Classification of First-Episode Schizophrenia Using Multimodal Brain Features: A Combined Structural and Diffusion Imaging Study. Schizophr Bull. 2019;45(3):591–9.

31. Venkataraman A, Whitford T, … CW-S, 2012 undefined. Whole brain resting state functional connectivity abnormalities in schizophrenia. Elsevier.

32. Wertz C, Hanlon F, Shaff N, … AD-S, 2019 undefined. Disconnected and Hyperactive: A Replication of Sensorimotor Cortex Abnormalities in Patients With Schizophrenia During Proactive Response Inhibition. academic.oup.com.

33. Meyer-Lindenberg A, Polin JB, Kohn PD, Holt JL, Egan MF, Weinberger DR, et al. Evidence for abnormal cortical functional connectivity during working memory in schizophrenia. Am J Psychiatry. 2001;158(11):1809–17.

34. Zhang M, Yang F, Fan F, Wang Z, Hong X, Clinical YT-N, et al. Abnormal amygdala subregional-sensorimotor connectivity correlates with positive symptom in schizophrenia. Elsevier.

35. Goswami S, Beniwal R, Kumar M, … TB-AJ of, 2020 undefined. A preliminary study to investigate resting state fMRI as a potential group differentiator for schizophrenia. Elsevier.

36. Woodward ND, Heckers S. Mapping Thalamocortical Functional Connectivity in Chronic and Early Stages of Psychotic Disorders. Biol Psychiatry. 2016 Jun;79(12):1016–25.

37. Lungu O, Barakat M, Laventure S, … KD-S, 2013 undefined. The incidence and nature of cerebellar findings in schizophrenia: a quantitative review of fMRI literature. academic.oup.com.

38. Beckmann CF, DeLuca M, Devlin JT, Smith SM. Investigations into resting-state connectivity using independent component analysis. Philos Trans R Soc B Biol Sci. 2005;360(1457):1001–13.

39. Calhoun VD, Adali T. Multisubject Independent Component Analysis of fMRI: A Decade of Intrinsic Networks, Default Mode, and Neurodiagnostic Discovery. IEEE Rev Biomed Eng. 2012;5:60–73.

40. Calhoun VD, de Lacy N. Ten Key Observations on the Analysis of Resting-state Functional MR Imaging Data Using Independent Component Analysis. Neuroimaging Clin N Am. 2017 Nov;27(4):561–79.

41. Joel SE, Caffo BS, Van Zijl PCM, Pekar JJ. On the relationship between seed-based and ICA-based measures of functional connectivity. Magn Reson Med. 2011 Sep;66(3):644–57.

42. Cole DM, Smith SM, Beckmann CF. Advances and pitfalls in the analysis and interpretation of resting-state FMRI data. Vol. 4, Frontiers in Systems Neuroscience. 2010.

43. … TG-3rd IC on C for, 2016 undefined. Resting state fMRI analysis using seed based and ICA methods. ieeexplore.ieee.org.

44. Wu L, Caprihan A, Bustillo J, Mayer A, NeuroImage VC-, 2018 undefined. An approach to directly link ICA and seed-based functional connectivity: Application to schizophrenia. Elsevier.

45. Society CG-E journal of the E, 1969 undefined. Investigating causal relations by econometric models and cross-spectral methods. JSTOR.

46. Wang X, Li F, Zheng H, Wang W, Zhang W, … ZL-S, et al. Breakdown of the striatal-default mode network loop in schizophrenia. Elsevier.

47. Guo W, Liu F, Xiao C, Yu M, Zhang Z, Liu J, et al. Increased causal connectivity related to anatomical alterations as potential endophenotypes for schizophrenia. ncbi.nlm.nih.gov.

48. Friston K. Statistical parametric mapping. 2014.

49. Gosset WS. Independent sample t tets. 1908.

50. Zhou B1, Tan C, Tang J CX. Brain functional connectivity of functional magnetic resonance imaging of patients with early-onset schizophrenia. pubmed.gov. 2010;35(1):17–24.

51. Dimitrios Asteriou SGH. VAR Model. In: Applied econometrics. 3rd ed. Red Globe Press; p. 552.

52. Mingrui Xia ,Jinhui Wang YH. BrainNet Viewer: A Network Visualization Tool for Human Brain Connectomics. 2013.

FIGURE LEGEND:

Figure 1 –Brain Activation in Schizophrenia Patients in Comparison with Healthy Individuals. Axial slices of activations in HC, TL, OL, and FL of: **(A)** healthy individuals (control), and **(B)** schizophrenia patients, at resting state. **(C)** Bar chart of average activations in ROIs for control and patients.

Figure 2 - Correlation Between ROIs in Schizophrenia. Person correlation between ROIs in **(A)** Control, **(B)** Schizophrenia patients. Connectivity in ROIs in **(C)** Control, and **(D)** Schizophrenia patients, using BrainNet Viewer (52).

Figure 3 – Structural Connectivity in ROIs. (A) Significant causality links in control between HC, OL, FL and TL, **(B)** Significant causality links in patients between HC, OL, FL and TL.

Figure 4– Structural Connectivity in ROIs obtained through Granger Causality for HC, OL, TL, and FL. Blue and Red arrows show significant granger causality between ROIs for the control case and SZ patients, respectively.

Figure 5 – Mediation Analysis in ROIs. (A) Significant mediation in control between HC, OL, and FL, **(B)** Significant mediation in patients between HC, OL, and FL.

TABLE LEGEND:

Table 1 - Estimated VAR Model for Control. "*Mod (1-4) at lag1*" is the VAR model till lag 1, $\hat{\beta}^{c}_{t-1}$ is the coefficient of variation for control case at lag 1, $\hat{\beta}^{c}_{t-2}$ is coefficient of variation for control case at lag 2, *t* is the test statistic, S.E is the standard error of the model, *p* value is the probability of obtaining test results by chance.

Mod (1-4) at lag1	$\hat{\beta}^{c}_{t-1}$	S.E	t	p	Mod (1-4), at lag 2	$\hat{\beta}^{c}_{t-2}$	S.E	t	p
HC(t) ← HC (t-1)	0.51	0.05	10.15	0.000	HC(t-2)	0.17	0.05	3.4	0.001
HC(t) ← OL (t-1)	0.15	0.07	2.14	0.032	OL(t-2)	-0.17	0.07	-2.5	0.011
HC(t) ← FL (t-1)	-0.00	0.09	-0.08	0.937	FL(t-2)	0.03	0.09	0.3	0.714
HC(t) ← TL (t-1)	-0.20	0.07	-2.62	0.009	TL(t-2)	0.16	0.07	2.1	0.036
OL(t) ← HC (t-1)	-0.05	0.03	-1.35	0.178	HC(t-2)	-0.02	0.03	-0.7	0.478
OL(t) ← OL (t-1)	0.73	0.05	13.61	0.000	OL(t-2)	0.01	0.05	0.2	0.832
OL(t) ← FL (t-1)	0.22	0.07	3.16	0.002	FL(t-2)	-0.11	0.07	-1.6	0.098
OL(t) ← TL (t-1)	0.04	0.05	0.75	0.456	TL(t-2)	0.04	0.06	0.7	0.453
FL(t) ← HC (t-1)	-0.01	0.03	-0.60	0.547	HC(t-2)	-0.00	0.03	-0.2	0.777
FL(t) ← OL(t-1)	-0.07	0.04	-1.66	0.098	OL(t-2)	0.05	0.04	1.1	0.234
FL(t) ← FL (t-1)	0.78	0.05	14.15	0.000	FL(t-2)	0.03	0.05	0.6	0.495
FL(t) ← TL (t-1)	0.09	0.04	2.02	0.043	TL(t-2)	0.01	0.04	0.4	0.681
TL(t) ← HC (t-1)	-0.05	0.03	-1.66	0.097	HC(t-2)	0.01	0.03	0.4	0.644
TL(t) ← OL (t-1)	0.12	0.04	2.58	0.010	OL(t-2)	-0.11	0.04	-2.3	0.020
TL(t) ← FL (t-1)	0.07	0.06	1.15	0.251	FL(t-2)	0.03	0.06	0.6	0.541
TL(t) ← TL (t-1)	0.67	0.05	12.46	0.000	TL(t-2)	0.11	0.05	2.1	0.035

Table 2 - Estimated VAR Model for Schizophrenia Patients. "*Mod (1-4) at lag1*" is the VAR model till lag 1, $\hat{\beta}^{p}_{t-1}$ is the coefficient of variation for patients at lag 1, $\hat{\beta}^{p}_{t-2}$ is coefficient of variation for patients at lag 2, *t* is the test statistic, S.E is the standard error of the model, *p* value is the probability of obtaining test results by chance.

Mod (1-4) at lag1	$\hat{\beta}^{p}_{t-1}$	S.E	t	p	Mod (1-4), at lag 2	$\hat{\beta}^{p}_{t-2}$	S.E	t	p
HC(t) ← HC (t-1)	0.36	0.05	6.34	0.000	HC(t-2)	0.29	0.05	5.0	0.000
HC(t) ← OL (t-1)	0.10	0.06	1.69	0.091	OL(t-2)	-0.01	0.06	-0.2	0.820
HC(t) ← FL (t-1)	-0.00	0.07	-0.10	0.917	FL(t-2)	0.03	0.07	0.4	0.638
HC(t) ← TL (t-1)	0.10	0.07	1.38	0.166	TL(t-2)	-0.11	0.07	-1.5	0.129
OL(t) ← HC (t-1)	0.09	0.04	1.96	0.050	HC(t-2)	-0.10	0.04	-2.04	0.042
OL(t) ← OL (t-1)	0.62	0.05	11.8	0.000	OL(t-2)	0.07	0.05	1.45	0.148
OL(t) ← FL (t-1)	-0.01	0.06	-0.22	0.826	FL(t-2)	0.03	0.06	0.58	0.562

OL(t) ← TL (t-1)	0.02	0.06	0.33	0.745	TL(t-2)	0.10	0.06	1.70	0.089
FL(t) ← HC (t-1)	-0.03	0.04	-0.65	0.513	HC(t-2)	0.05	0.04	1.14	0.256
FL(t) ← OL (t-1)	0.13	0.05	2.65	0.008	OL(t-2)	-0.02	0.05	-0.40	0.693
FL(t) ← FL (t-1)	0.31	0.06	5.10	0.000	FL(t-2)	0.25	0.06	4.21	0.000
FL(t) ← TL (t-1)	0.14	0.06	2.39	0.017	TL(t-2)	-0.01	0.06	-0.27	0.789
TL(t) ← HC (t-1)	-0.06	0.04	-1.47	0.142	HC(t-2)	-0.01	0.04	-0.30	0.768
TL(t) ← OL (t-1)	0.03	0.04	0.76	0.449	OL(t-2)	0.09	0.04	1.93	0.053
TL(t) ← FL (t-1)	0.02	0.05	0.46	0073	FL(t-2)	-0.06	0.05	-1.13	0.259
TL(t) ← TL (t-1)	0.69	0.05	12.3	0.000	TL(t-2)	0.21	0.05	3.86	0.000

Table 3: Granger Causality Wald Test for Control. Equation is a dependent variable while excluded is representing independent variable,chi^2 is a test of association ,df stands for degree of freedom, Prob>chi^2 is the probability value for drawing conclusion about null hypothesis.

Equation	Excluded	Chi^2	df	Prob>chi^2
HC	OL	6.628	2	0.036
	FL	0.223	2	0.894
	TL	6.970	2	0.031
	ALL	13.056	6	0.042
OL	HC	6.265	2	0.044
	FL	11.206	2	0.004
	TL	3.815	2	0.148
	ALL	30.024	6	0.000
FL	HC	1.171	2	0.557
	OL	2.751	2	0.253
	TL	10.839	2	0.004
	ALL	15.068	6	0.020
TL	HC	3.450	2	0.178
	OL	7.001	2	0.030
	FL	6.353	2	0.042
	ALL	19.55	6	0.003

Table 4 – Granger Causality Wald Test for Patients. Equation is a dependent variable while excluded is representing independent variable chi^2 is a test of association ,df stands for degree of freedom, Prob>chi^2 is the probability value for drawing conclusion about null hypothesis.

Equation	Excluded	Chi^2	df	Prob>chi^2
HC	OL	3.977	2	0.137
	FL	0.231	2	0.891
	TL	2.383	2	0.304
	ALL	10.302	6	0.112
OL	HC	5.218	2	0.074
	FL	0.337	2	0.845
	TL	10.669	2	0.005

	ALL	29.205	6	0.000
FL	HC	1.294	2	0.524
	OL	9.596	2	0.008
	TL	13.135	2	0.001
	ALL	38.862	6	0.000
TL	HC	3.747	2	0.154
	OL	10.069	2	0.007
	FL	1.273	2	0.529
	ALL	13.544	6	0.035

Table 5 – Mediation Analysis for Regions of Interest. S.E. stands for standard error, C.R. is the confidence ratio and P is the probability value.

	Dependent	Effect	Independent	Estimate	S.E.	C.R.	P
Control	HC	<---	OL	-0.048	0.045	-1.062	0.288
	FL	<---	OL	0.476	0.035	13.791	***
	FL	<---	HC	0.225	0.038	5.904	***
Patients	**Dependent**	**Effect**	**Independent**	**Estimate**	**S.E.**	**C.R.**	**P**
	HC	<---	OL	0.39	0.038	10.333	***
	FL	<---	OL	0.464	0.035	13.098	***
	FL	<---	HC	0.361	0.042	8.676	***

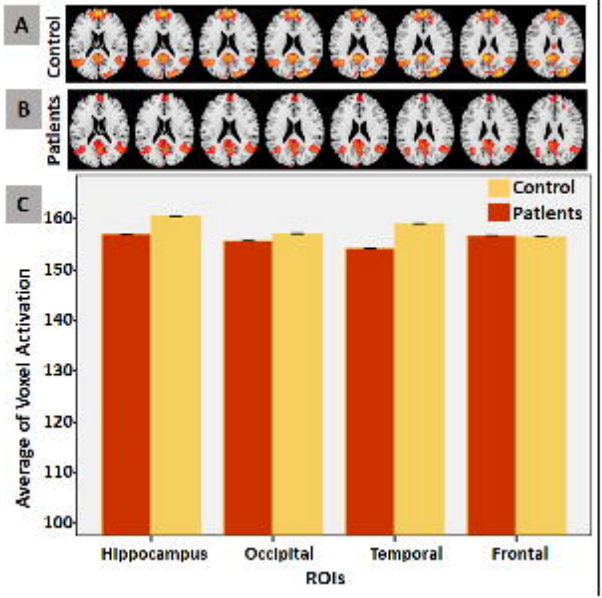
A
Control
B
Patients
C
Control
Patients
160
150
140
130
120
110
100
Average of Voxel Activation
Hippocampus
Occipital
Temporal
Frontal
ROIs

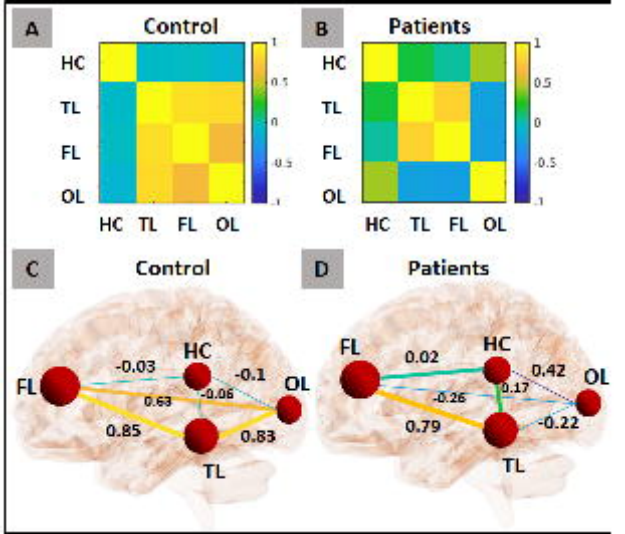
A
Control
HC
TL
FL
OL
HC TL FL OL
1
0.5
0
-0.5
-1
B
Patients
HC
TL
FL
OL
HC TL FL OL
1
0.5
0
-0.5
-1
C
Control
FL
HC
OL
TL
-0.03
-0.1
-0.06
0.63
0.85
0.83
D
Patients
FL
HC
OL
TL
0.02
0.42
0.17
-0.26
0.79
-0.22

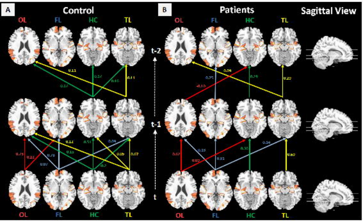
A
Control
OL
FL
HC
TL
B
Patients
Sagittal View
t-2
t-1
t
OL
FL
HC
TL

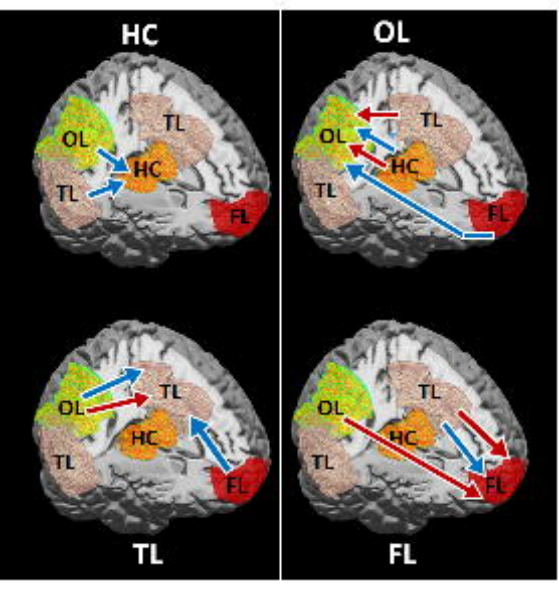
HC
OL
TL
HC
TL
FL
OL
TL
OL
HC
TL
FL
TL
OL
HC
TL
FL
TL
OL
TL
HC
TL
FL
FL

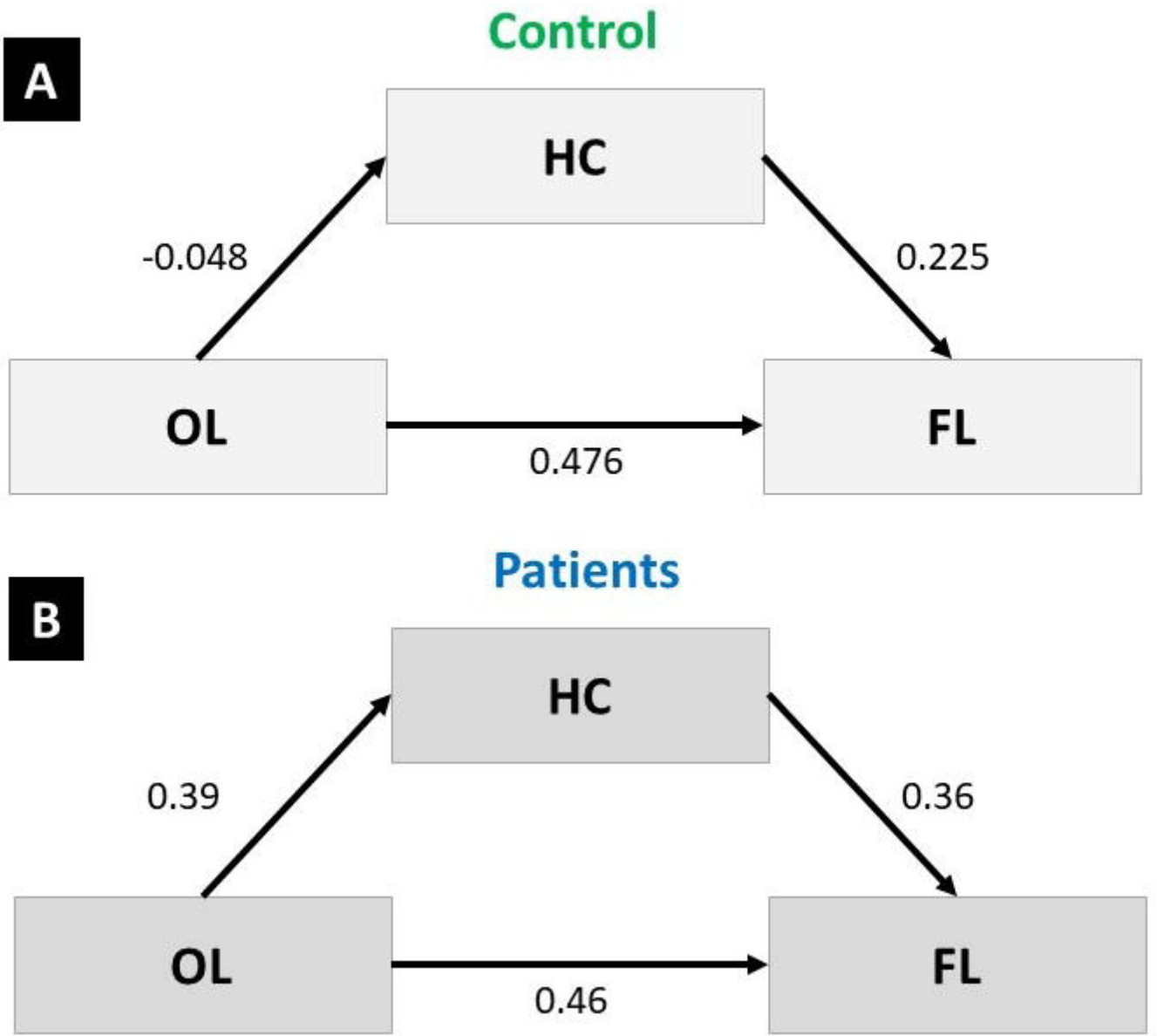
A
Control
HC
-0.048
0.225
OL
FL
0.476
B
Patients
HC
0.39
0.36
OL
FL
0.46